

Poly(96L/4D-Lactide) implants for repair of orbital floor defects: an *in vitro* study of the material properties in a simulation of the human orbit

F. W. CORDEWENER*, F. R. ROZEMA*, C. A. P. JOZIASSE‡, R. R. M. BOS*, G. BOERING*, A. J. PENNING‡

*Department of Oral and Maxillofacial Surgery, University Hospital Groningen, The Netherlands

‡Department of Polymer Chemistry, University of Groningen, The Netherlands

To test the mechanical and physical properties of two types of poly(96L/4D-lactide) (PLA96) implants and to evaluate their suitability for repair of large orbital floor defects, a study using an *in vitro* set-up was performed. Implants, 0.2 mm thick and 28 mm in diameter, were produced by either an extrusion process (type A) or by direct machining (type B) and had a molecular weight (M_w) of 64×10^3 and 146×10^3 g/mole, respectively, after γ -sterilization with a dose of 25 kGy. The implants were tested over 8 weeks in an apparatus simulating the human orbit with a 3.1 cm² orbital floor defect under a static load corresponding to a retrobulbar pressure of 13 mm Hg as well as unloaded. Both implant types were able to counteract the applied static load without fracturing or excessive sagging. The type A implants sagged more than the type B implants (2.3 ± 0.1 mm versus 1.0 ± 0.0 mm, $p < 0.01$) but retained and even increased their strength during the study whereas the type B implants showed a gradual strength-loss. In the clinical setting the observed sagging in both types would not have resulted in positional changes of the eyeball. It is concluded that with respect to the mechanical properties, both types of PLA96 implants tested are suitable for repair of large orbital floor defects.

1. Introduction

Enophthalmos and diplopia are the most-often encountered sequelae of orbital floor fractures. Early surgical intervention is required in case of manifest enophthalmos of 2–3 mm or more and large orbital floor fractures likely to result in late enophthalmos. Early surgical intervention is also required in case of symptomatic diplopia caused by extraocular muscle dysfunction due to tissue incarceration [1–4]. The aim of surgical intervention should be to reposition prolapsed orbital contents, to release incarcerated orbital tissue and to reconstruct the orbital floor in its correct anatomical position [5–9]. To reconstruct a large orbital floor defect and support the orbital contents the aid of an implant will frequently be needed [2, 7]. For this purpose, the use of a resorbable alloplastic material presents an appealing choice. When healing of the defect is complete, the support of the implant will no longer be required. Subsequent resorption of the implant material should obviate complications regularly reported such as infection, orbital hemorrhage, and migration or extrusion which are often related to the life-long presence of non-resorbable materials [10–13]. In addition, the use of an alloplastic material obviates the need for a donor-site operation for harvesting bone and provides the

opportunity of adapting the mechanical properties and resorption characteristics of the implant as required [14–16].

The success after reconstruction of a large orbital floor defect will, to a large extent, depend on the mechanical properties of the implant used. With respect to these properties, two factors are considered to be of major importance. First, an orbital floor implant should have sufficient form stability to avoid excessive sagging or deformation and, second, it should be strong enough to counteract the load it is subjected to [17–19]. In addition, a resorbable implant should retain its strength long enough for the floor defect to heal properly.

Available alloplastic resorbable materials such as Polyglactin and Gelfilm[®] should only be used for the repair of small defects because of their insufficient mechanical properties and rapid resorption [14, 15]. Polydioxanone (Ethicon[®], Sommerville, NJ) implants have better mechanical properties but are fairly bulky and will not always prevent postoperative enophthalmos after repair of large defects [20]. In our department, Rozema *et al.* successfully used orbital floor implants of as-polymerized poly(L-lactide) (PLLA) in preclinical and clinical studies [21]. However, the degradation rate of PLLA is very low and in the long

term PLLA may evoke an unfavourable tissue response [22, 23].

Based on these findings, we have made orbital floor implants of poly(96L/4D-lactide) (PLA96). The initial mechanical properties of PLA96 are comparable to those of PLLA [24] but it shows a higher degradation rate [24, 25] and may show easier resorption without late complications. Our primary interest was whether these PLA96 orbital floor implants could meet the requirements concerning the mechanical properties needed for successful reconstruction of a large orbital floor defect. Because, to our knowledge, the open literature does not provide quantitative data concerning these requirements, we used an *in vitro* set-up with the aim of testing the mechanical and physical properties of two types of PLA96 implants and to evaluate their suitability for the repair of large orbital floor defects.

2. Materials and methods

2.1. PLA

As-polymerized poly(96L/4D-lactide) (PLA96) was prepared by DSM-Research, Geleen, The Netherlands. Polymerization of L- and D-lactide (mole ratio 96/4) was performed in bulk under vacuum for 68 h at 120°C. Stannous-octoate 0.02 wt% was used as a catalyst. The weight-average molecular weight (\bar{M}_w) of the PLA96 was 1800×10^3 g/mole relative to polystyrene standards.

2.2. Implant production

Two types of PLA96 implants were produced, both 0.2 mm thick and 28 mm in diameter (Fig. 1). The first, type A, were produced by extruding the granulate of a cryogenically ground block of as-polymerized PLA96 to a foil 0.2 mm thick at 200°C that was wound on a hot roller at 80°C, and by subsequent punching. The second, type B, were machined directly from a block of as-polymerized PLA96. After production, the type A implants had a \bar{M}_w of 177×10^3 g/mole and were translucent while the type B implants had a \bar{M}_w of 1210×10^3 g/mole and were

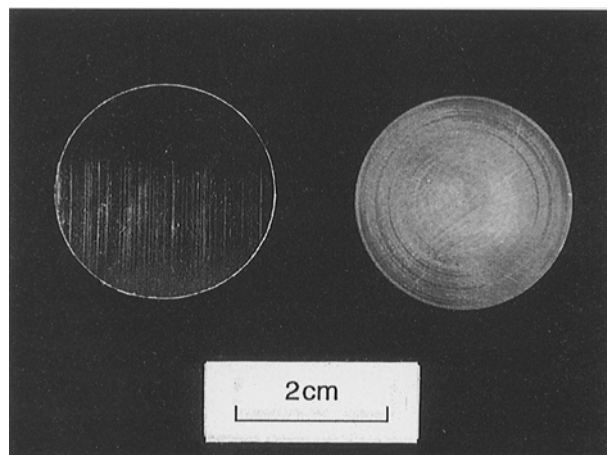


Figure 1 Photograph of a type A (left) and type B (right) orbital floor implant.

whitish opaque. Each implant was weighed and separately packed in a paper/PE/PP laminate bag (P3 'DRG Hospital supplies'). Subsequently, the implants were sterilized by γ -irradiation with a dose of 25 kGy.

2.3. Sterilization effects

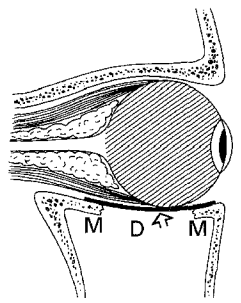
To detect possible changes of the initial material properties of the implants due to the γ -irradiation sterilization procedure, four implants of both type A and type B were characterized before and after sterilization.

2.4. Experimental procedure

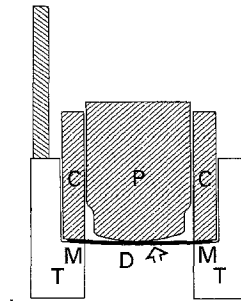
An *in vitro* set-up was used to monitor the "post-operative" performance of an orbital floor implant in time after repair of a large "orbital floor defect". The set-up allows the sagging, load at break and displacement at break of the implant under test to be measured. The main component within this set-up is an apparatus simulating the human orbit with a fractured orbital floor (Fig. 2). The apparatus consists of three separate parts. The first part is a round perspex tray (T) representing the orbital floor with a defect (D) surrounded by an intact margin (M). The second and third part represent the orbital contents and comprise a round stainless steel cylinder (C) and stainless steel plunger (P), which can slide up and down freely in cylinder C.

The design of the apparatus was based on literature concerning the anatomy and physiology of the human orbit and the epidemiology of orbital floor fractures [7, 8, 26–31]. Defect D in the perspex tray had a diameter of 2 cm, the area size of the defect thus being 3.1 cm². The surrounding margin M was 5 mm wide, its area size being 3.9 cm², and had a down-slope of 1 mm towards the centre of the tray. Plunger P and cylinder C subjected the implant under test in the apparatus to a load of 125 g, which corresponds to an intraorbital pressure or retrobulbar pressure (RBP) of 13 mm Hg. The 125 g load was divided over the covered defect (55 g) and the margin (70 g) according to the ratio of their respective area size. Plunger P had a rounded-off working end ($r = 30$ mm) and its diameter was reduced from 20 mm to 18 mm over a length of 10 mm from the working end. The underside of cylinder C was bevelled so as to adapt the sloping margin of the perspex tray. The apparatus was equipped with a stainless steel calibration rod (R) fitted in the wall of the perspex tray.

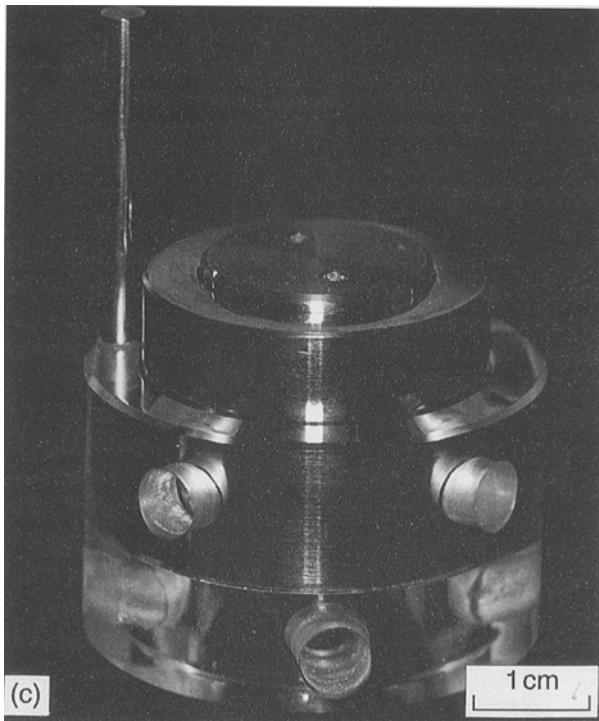
The type A and type B implants were tested separately in two consecutive experiments with a duration of 8 weeks under identical experimental conditions. Both implant types were simultaneously tested under static load in the apparatus as well as unloaded to examine the effects of the load on the mechanical and physical properties of the implants. To test the implants under load, 16 of the described apparatus were used. Defect D was covered with a PLA96 implant centred carefully to ensure equal coverage of the surrounding margin. Subsequently, plunger P and cylinder C were put on the centre and the margin of the



a



b



(c)

Figure 2 (a) Schematic representation of the human orbit with its contents. The orbital floor shows a defect (D) which is surrounded by intact margin (M). An orbital floor implant (arrow) is covering the defect, extending over the margin and supporting the orbital contents. (b) Schematic representation of the apparatus simulating the human orbit with its contents. The perspex tray (T) represents the orbital floor with a defect (D). An orbital floor implant (arrow) is covering the defect, extending over margin (M) and supporting stainless steel cylinder (C) and plunger (P) which represent the orbital contents. (c) Photograph of the apparatus.

implant. Another 16 implants were mounted in a plastic rack without being subjected to any load. The 16 apparatus and the rack were submerged in a lightly stirred temperature-controlled bath containing 10 l of a 0.1 M phosphate buffer (pH 7.4) to which was added an antimicrobial agent ($\text{Na}_2\text{HPO}_4 + \text{KH}_2\text{PO}_4 + 0.02 \text{ wt}\% \text{ NaN}_3$) at a testing temperature (T_t) of 37°C .

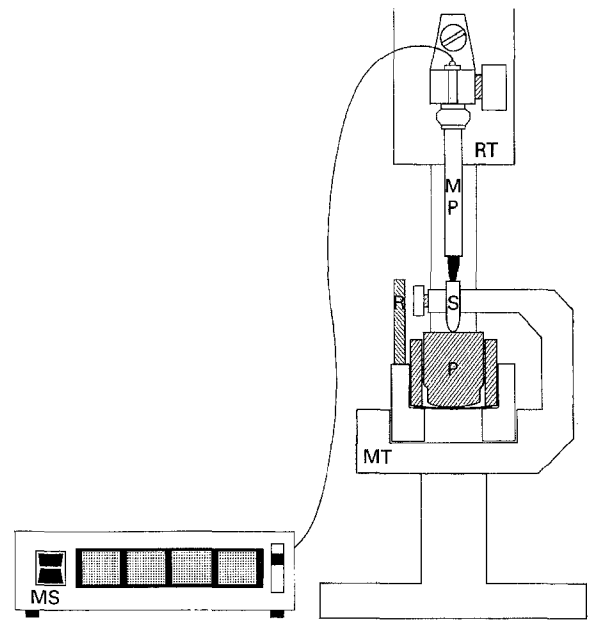


Figure 3 Arrangement for measuring sagging of the loaded orbital floor implants. The apparatus is secured on mounting table (MT) of the measuring stand. Stainless steel pin (S) is lowered to the top centre of plunger (P) and secured by a locking screw. First, measuring probe (MP), fitted to the rotatable top part (RT) of the measuring stand, is put on top of the apparatus's calibration rod (R) and the display of the connected Sony magnescale (MS) set for 0. Subsequently, the measuring probe is rotated to the top centre of pin S and the offset from the 0 reading recorded.

2.5. Implant characterization

Sagging of the loaded implants was measured at weekly intervals on the same four apparatus. For this purpose, the apparatus were temporarily retrieved from the phosphate buffer and mounted in a measuring stand (CEJ 531-1, Eskilstuna, Sweden). Subsequently, the vertical distance between the top centre of plunger P and the top of calibration rod R was measured on a Sony (Sony Magnescale Inc. Japan) magnescale LY-101 (Fig. 3).

At 2, 4, 6 and 8 weeks after the start of the experiment four apparatus with loaded implants and four unloaded implants were retrieved from the phosphate buffer. After visual examination each implant was weighed ($= m_{\text{wet}}$) separately after drying off the adherent moisture with a tissue.

To measure displacement and load at break the loaded implants were replaced in their respective apparatus after weighing and only the cylinders put back on. The plungers were not replaced. The apparatus were then mounted in an Instron 4301 testing machine equipped with a stainless steel plunger fitted to a 5 kN or 100 N load cell. This plunger with rounded off end ($r = 25 \text{ mm}$) and diameter of 16 mm was put on the surface centre of the implant. Subsequently, the plunger was pushed through the implant at a cross-head speed of 1 mm/min. The unloaded implants were measured using the same procedure after changing the remains of the loaded implants for the unloaded implants. The remains of all tested implants were vacuum dried at 40°C to constant weight.

Water absorption of the retrieved implants was calculated using the formula: $\% \text{H}_2\text{O} = 100 (m_{\text{wet}} - m_{\text{dry}}) / m_{\text{dry}}$, in which m_{dry} is mass after drying

TABLE I Mechanical and physical properties of type A and type B PLA96 orbital floor implants before and after γ -irradiation sterilization

Implant type	Displacement at break (mm)	Load at ^a break (N)	Molecular ^b weight ($\bar{M}_w \times 10^3$)	Heat of ^b fusion (J/g)	Melting ^b temperature (°C)	Glass transition ^b temperature (°C)
A unsterilized	(4) ^c	(98) ^c	177	25	154.4	52.5
A sterilized	3.2 ± 0.3	70.8 ± 7.7	64	29.8	156.9	51.6
B unsterilized	3.1 ± 0.8	199.1 ± 61.4	1210	33.4	159.2	56.8
B sterilized	2.2 ± 0.2 ^d	152.7 ± 70.2	146	37.7	157.8	55.4

^a Values are mean ± SD for four implants

^b Values for one implant

^c No break occurred; data are an estimate of the value immediately before folding of the implants into the defect

^d $p < 0.01$ versus type A sterilized

to constant weight. Change in mass (Δm) was calculated using the formula: $\Delta m = 100(m_{dry} - m_0)/m_0$, in which m_0 is initial dry mass at the start of the study. \bar{M}_w was determined by gel permeation chromatography (GPC). GPC samples (1–3 mg/ml) were measured in chloroform on a Spectra Physics AS1000 (PSS 5 μ SDV 1000 Å and 10⁵ Å, Shodex RI71, Viskotek H502) relative to narrow polystyrene standards. Thermal properties were measured by differential scanning calorimetry (DSC) on a Perkin Elmer DSC-7. DSC samples (5–10 mg) were heated at a scanning rate of 10°C/min. GPC and DSC analyses were performed on samples of one of the loaded and unloaded implants retrieved at each time interval.

2.6. Data analysis

Data are given as mean ± SD. A two-tailed *t*-test was used to analyse all data at a level of rejection of 0.05. To avoid random significances, *p*-values were adjusted for the number of tests performed. All analyses were performed with SPSS/PC⁺™.

3. Results

3.1. Sterilization effects (Table I)

The non-sterilized type A implants did not break during the push-through test. Instead, the implants folded and were merely pushed down into the hole in the perspex tray. For these implants, therefore, data for displacement and load at break could not be obtained. The sterilized type A implants all broke during the push-through test. The γ -irradiation sterilization procedure did not significantly ($p > 0.05$) change the initial values for displacement and load at break of the type B implants. \bar{M}_w , however, was seriously reduced. \bar{M}_w of the type A implants was decreased by more than 60% while \bar{M}_w of the type B implants was decreased by nearly 90%. Heat of fusion (ΔH_m) of both implant types was somewhat increased whereas melting temperature (T_m) and glass transition temperature (T_g) were only minimally affected.

3.2. Implant characterization

3.2.1. Loaded implants

Both implant types sagged under load but none of the implants fractured spontaneously during the test

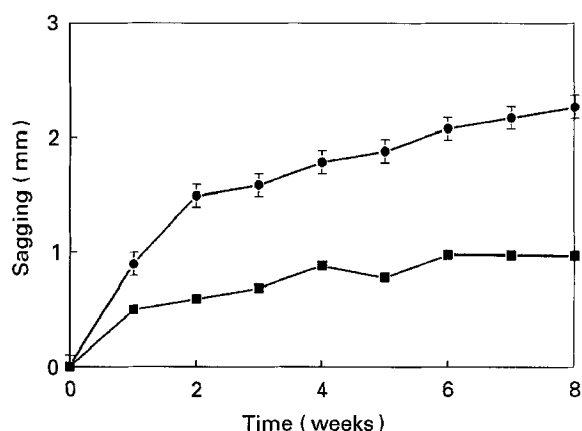


Figure 4 Sagging of PLA96 orbital floor implants as a function of time under static load: ● type A; ■ type B. Values are mean ± SD for four implants. If not depicted, SD is within symbol range.

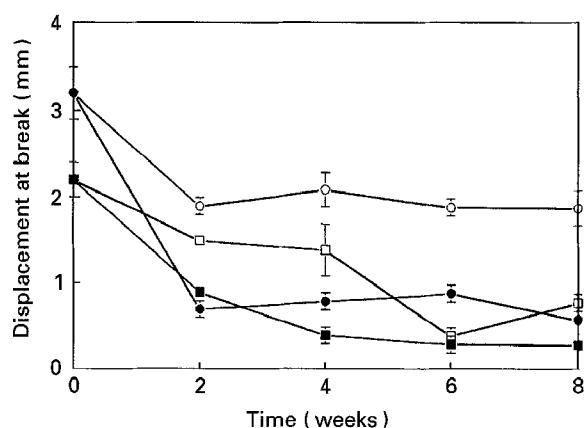


Figure 5 Displacement at break of PLA96 orbital floor implants as a function of time under static load and unloaded: ● type A loaded; ■ type B loaded; ○ type A unloaded; □ type B unloaded. Values are mean ± SD for four implants. If not depicted, SD is within symbol range.

period. For both implant types about 50% of the sagging occurred during the first 2 weeks (Fig. 4). While sagging of the type A implants continued to increase with time, no further sagging of the type B implants was observed from week 6. At the end of the test period, sagging of the type A implants was more than twice that of the type B implants (2.3 ± 0.1 mm versus 1.0 ± 0.0 mm, $p < 0.01$).

A distinct difference between the implant types was observed for displacement at break (Fig. 5). Displacement of the type A implants was decreased by nearly

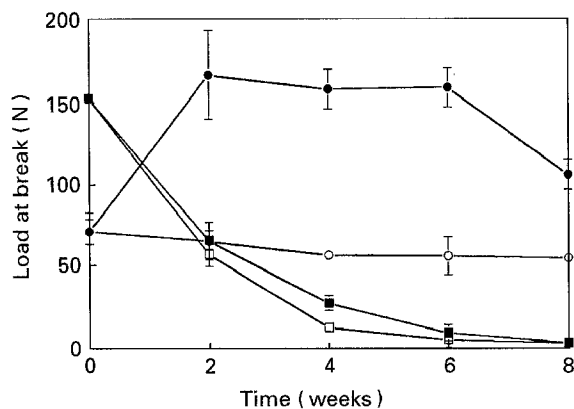


Figure 6 Load at break of PLA96 orbital floor implants as a function of time under static load and unloaded: ● type A loaded; ■ type B loaded; ○ type A unloaded; □ type B unloaded. Values are mean \pm SD for four implants. If not depicted, SD is within symbol range.

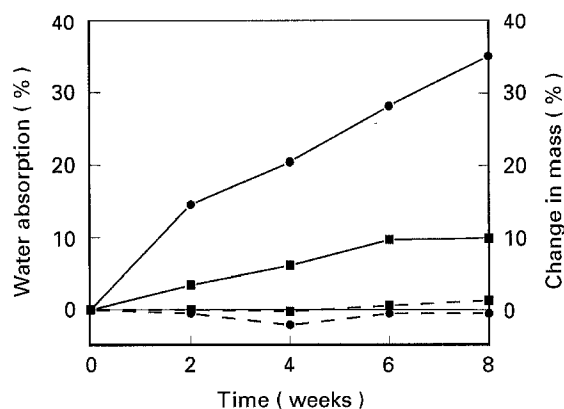


Figure 7 Water absorption (—) and change in mass (----) of PLA96 orbital floor implants as a function of time under static load: ● type A; ■ type B. Values are mean \pm SD for four implants. If not depicted, SD is within symbol range.

80% at week 2 and subsequently remained virtually unchanged, whereas displacement of the type B implants showed a continuous gradual decrease until week 8.

In contrast to the observation for displacement at break, load at break of the type A implants was increased by about 100% at week 2 ($p < 0.01$) (Fig. 6). This level was maintained until week 6 before it started to decrease. Load at break of the type B implants was decreased by more than 50% during the first 2 weeks and subsequently continued to gradually decrease. At the end of the test period the type B implants had become very fragile.

Water absorption occurred at a fairly constant rate for both implant types (Fig. 7). At week 8 water absorption of the type A implants was about 3.5 times that of the type B implants ($35.2 \pm 0.4\%$ versus $9.9 \pm 0.3\%$, $p < 0.01$). The mass of both implant types showed only minor changes (Fig. 7). At week 8 a mass-loss of $1.3 \pm 0.1\%$ was measured in the case of the type B implants.

\bar{M}_w of both implant types, the type B implants in particular, was decreased rapidly during the first 2 weeks (Fig. 8). With \bar{M}_w of the type B implants remaining somewhat higher than that of the type

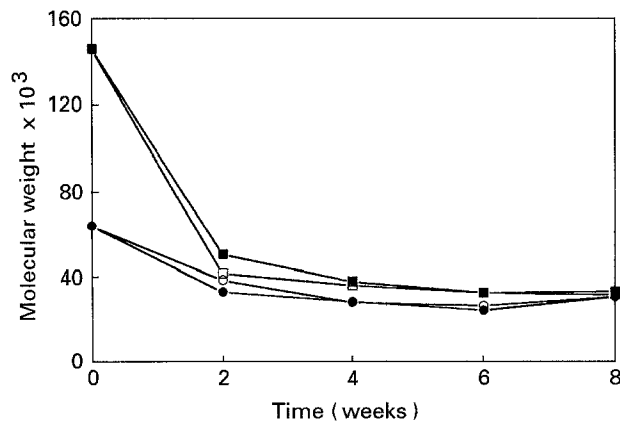


Figure 8 Molecular weight of PLA96 orbital floor implants as a function of time under static load and unloaded: ● type A loaded; ■ type B loaded; ○ type A unloaded; □ type B unloaded. Values are for one implant.

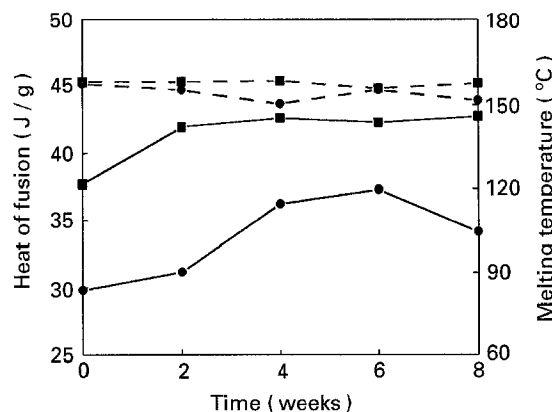


Figure 9 Heat of fusion (—) and melting temperature (----) of PLA96 orbital floor implants as a function of time under static load: ● type A; ■ type B. Values are for one implant.

A implants, \bar{M}_w of both implant types continued to decrease at a low rate.

ΔH_m of both implant types was increased by approximately 5 J/g in 8 weeks, with ΔH_m of the type A implants remaining lower than that of the type B implants during the entire test period (Fig. 9). T_m of the type A implants was decreased from 156.9°C to 150.6°C in 8 weeks, while T_m of the type B implants remained practically unchanged (Fig. 9).

T_g of both type A and type B implants was decreased slightly during the test period, by 4.5°C and 2.9°C , respectively.

3.2.2. Unloaded implants

Some of the unloaded type A implants and, to a lesser extent, unloaded type B implants lost their initial planeness and became somewhat bulged or curled.

Displacement of the unloaded type A implants showed a pattern similar to that of the loaded type A implants (Fig. 5). The decrease at week 2, however, was only about half the decrease of the loaded type A implants. Displacement of the unloaded type B implants gradually decreased like the loaded type B implants but somewhat less rapidly.

Unlike the loaded type A implants, load at break of the unloaded type A implants did not increase but

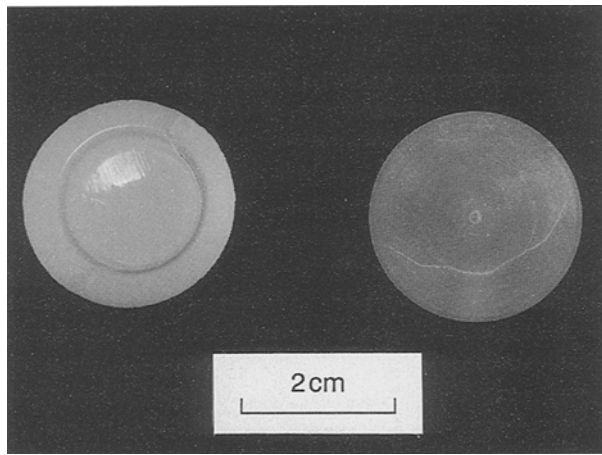


Figure 10 Photograph of a type A (left) and a type B (right) implant after 8 weeks under load in the apparatus. The total sagging of the type A implants was more than twice that of the type B implants. Note the whitish opaque appearance of the type A foils, in contrast to their initial translucency.

instead showed a slow, gradual decrease (Fig. 6). Load at break of the unloaded type B implants decreased in a pattern similar to the loaded type B implants.

The measurements for water absorption of both unloaded implant types were not significantly ($p > 0.05$) different from those of the loaded implants. At week 8, an increase in mass of $1.0 \pm 0.1\%$ was measured for the unloaded type A implants whereas the mass-loss measured for the unloaded type B implants was lower than that of the loaded type B implants ($0.5 \pm 0.1\%$ versus $1.3 \pm 0.1\%$, $p < 0.01$).

For both unloaded implant types no obvious differences between \bar{M}_w of the loaded and unloaded implants were measured (Fig. 8).

The measurements for ΔH_m , T_m and T_g of both unloaded implant types were practically the same as for the loaded implants.

The type A implants, both loaded and unloaded, had lost their initial translucency and had changed to whitish opaque within the first 2 weeks of the test period. The type B implants did not change appearance notably during the entire test period (Fig. 10).

4. Discussion

The results of this study show that both PLA96 implant types tested were able to counteract the load they were subjected to during an 8 week period without fracturing or excessive sagging. The type A implants sagged more than the type B implants but retained and even increased their strength during the study whereas the type B implants showed a gradual strength-loss.

The *in vitro* set-up used in this study appears to be a helpful, objective method to study the mechanical and physical properties of orbital floor implants and to get a good impression of their usefulness in the clinical setting with respect to these properties. The apparatus from the *in vitro* set-up was designed on the basis of literature concerning the anatomy and physiology of the human orbit and the epidemiology of orbital floor fractures [7, 8, 26–32]. Literature con-

cerning the load acting on an orbital floor in normal conditions or after reconstruction was found to be scarce. The only relevant data in this respect concerned the intraorbital pressure or retrobulbar pressure (RBP) [27–31].

Defects of the orbital floor range in size from 1 to 4 cm² and enophthalmos is usually present or likely to develop when the defect is larger than half of the orbital floor or over 2.5 cm² in area [7, 8]. An orbital floor implant used for repair of the defect should extend a few millimetres over the intact margins around the entire defect to ensure its stability [26]. In normal conditions, the RBP in humans ranges from 3 to 4.5 mm Hg [27, 28]. This normal RBP can increase by approximately 2 mm Hg due to functional eye movements [28–30]. In addition, external pressure on the eyeball can result in peak increases of the RBP to more than 30 mm Hg [31]. We decided to subject the implant in the apparatus to a load corresponding to twice the RBP that, according to available data, would exist in the human orbit with normal eye function, i.e. $(4.5 + 2) \times 2 = 13$ mm Hg. The load an orbital floor is subjected to by the orbital contents is distributed equally over the entire orbital floor area. Therefore, the load was divided over the covered defect and the margin according to the ratio of their respective area size.

During the 8 week test period, both implant types sagged under load. Voluminal changes of the orbit can result in changes of the eyeball position. For notable changes of the eyeball position a change in volume in the human orbit of at least 2 to 3 cm³ is required [1, 3, 32]. The total sagging of the type A implants of 2.3 mm corresponds to an increase in volume of less than 0.5 cm³. Therefore, the amount of sagging observed would in the clinical setting not have resulted in positional changes of the eyeball.

A distinct difference was observed between the measurements for displacement and load at break of both implant types. It is difficult to relate these measurements to possible implications for the clinical setting. The strength of a human orbital floor varies largely. Jo *et al.* found, in a study on resected and macerated human orbital floors, the ultimate strength to vary from 0.9 to 6.6 N/mm² [33]. This strength variation can be explained from anatomical variations of the human orbital floor. Its area ranges in size from 3 to 5 cm² and the thickness of the bone varies from 0.1 to 1 mm [34, 35]. Sometimes, natural dehiscences occur in the bony orbital floor [36]. However, over the entire spectrum of anatomical variation the position and function of the eye may be completely normal and undisturbed, even after removal of the bony orbital floor [5, 37]. In addition, it is difficult to establish how long it takes before an orbital floor defect may be considered healed and strong enough to provide adequate support to the orbital contents without the risk of adverse sequelae in the long term, such as late enophthalmos or diplopia. After repair of an orbital floor defect with a resorbable implant, strength-loss of the implant due to its degradation will presumably be compensated for by the formation of fibrous connective tissue and bone during the healing process.

In our department, Rozema *et al.* studied 0.4 mm thick PLLA orbital floor implants in goats. Twelve weeks postoperatively a dense connective tissue capsule was observed on the orbital side of the implant and after 19 weeks a progressive bony plate was observed which partially covered the implant [21]. Cutright *et al.* repaired orbital floor defects in monkeys with 1.5 mm thick PLA sheets. Eight weeks postoperatively they observed bone remodelling in apposition of a fibrous connective tissue capsule surrounding the implant [38]. In a number of other *in vivo* animal studies on resorbable alloplastic implants like Iyodura, Gelfilm® and polyglactin, fibrous connective tissue formation followed by the onset of bone formation was observed between 6 and 12 weeks after implantation [14–16]. Based on these findings we assumed that a resorbable orbital floor implant should retain enough strength to support the orbital contents for a period of approximately 6 to 12 weeks. By this time the fibrous connective tissue layer, together with newly formed bone, will be strong enough to provide adequate support of its own. At the end of our study, load at break turned out to be 108 N for the type A implants and 3.5 N for the type B implants. This corresponds to pressures of approximately 4100 mm Hg and 130 mm Hg, respectively. Therefore, after 8 weeks both implant types tested still had retained enough strength to counteract the 125 g load or a 13 mm Hg RBP.

The observed difference in mechanical performance between the two implant types, especially during the first 2 weeks, most probably results from differences in physical structure caused by the different processing methods of the implants. The type A implants were punched from a larger foil produced by an extrusion process. The extrusion process had to be performed at a temperature of approximately 200 °C because of the high T_m of PLA96 ($T_m = 156$ °C). This high extrusion temperature may have led to thermal degradation. After the extrusion process, the type A implants had both a lower \bar{M}_w and ΔH_m than the machined type B implants, indicating a lower degree of crystallinity. In addition, the T_g of the type A implants was found to be lower than of the type B implants and relatively close to the testing temperature (T_t) of 37 °C. In fact, T_t was in the onset of the glass transition trajectory of the type A implants, which implies that the amorphous phase of these implants was entering the rubbery state. Under static load, therefore, the type A implants exhibited a more ductile behaviour than the type B implants. During ductile deformation, the polymer chains in the amorphous zones become stretched and oriented. This results in an increase of elastic modulus (E) and strength of the material, which is even enhanced by the increase in crystallinity as degradation proceeds. Under static load the material properties of the implant material can thus change. Since the type A implants were most prone to changes in material properties due to the static load, these showed larger differences in mechanical performance between the loaded and the unloaded implants than in the case of the type B implants. Water absorbed in the amorphous zones may cause plasticization. The fairly high rate of water absorption may, therefore,

have added to the ductile behaviour of the type A implants.

The difference in physical structure may also explain the differences observed in the effect of the γ -irradiation sterilization procedure on the initial material properties of the implants. The fact that \bar{M}_w of the type B implants was more seriously affected than that of the type A implants may have been due to their higher degree of crystallinity. The polymer chains in the amorphous zones tying the crystallites together are particularly prone to scissioning by γ -irradiation [39]. Loss of tie-chains in the amorphous zones can result in strength-loss of the material before the onset of mass-loss [40, 41]. Despite the serious reduction of \bar{M}_w of the type B implants, however, \bar{M}_w apparently remained high enough to ensure sufficient initial mechanical properties.

From the results of this study it can be concluded that, with respect to the mechanical properties, both types of PLA96 implants tested are suitable for the repair of large orbital floor defects. Both PLA96 implant types were able to counteract the load they were subjected to during an 8 week period without fracturing or excessive sagging. In the clinical setting the amount of sagging observed would not have resulted in positional changes of the eyeball. After 8 weeks, both implant types tested still had retained enough strength to counteract the 125 g load or a 13 mm Hg RBP. When comparing the type A and the type B implants, the A implants appear to be preferable considering their better strength retention and their relative ease of production.

The PLA96 implants combine good mechanical properties with limited thickness. Because of the good mechanical properties, the implants are suitable for the repair of large orbital floor defects. Moreover, because of the implants' limited thickness, large orbital floor defects can be reconstructed in their correct anatomical position without disturbing the spatial relationships in the orbit.

Successful treatment of an orbital floor defect depends not only on the mechanical properties of the implant used: other factors such as the tissue reaction to and the resorption characteristics of the implants should also be evaluated and taken into consideration. Consequently, further study on these subjects is needed.

Acknowledgements

The authors wish to thank Mr H.J. van den Berg and Mrs M. Lammers of DSM-Research, Geleen for their assistance in the implant production and Mr A.B. Verwey from the Department of Polymer Chemistry, University of Groningen for his technical assistance in the implant characterization.

References

1. P. N. MANSON, A. GRIVAS, A. ROSENBAUM, M. VAN-NIER, J. ZINREICH and N. ILIFF, *Plast. Reconstr. Surg.* **77** (1986) 203.
2. J. DUTTON, *Surv. Ophthalmol.* **35** (1991) 279.
3. P. N. MANSON and N. ILIFF, *ibid.* **35** (1991) 280.

4. A. M. PUTTERMAN, *ibid.* **35** (1991) 292.
5. B. SMITH, R. D. LISMAN, J. SIMONTON and R. DELLA ROCCA, *Plast. Reconstr. Surg.* **74** (1984) 200.
6. R. B. WILKINS and W. E. HAVINGS, *Ophthalmology* **89** (1982) 464.
7. M. J. HAWES and R. K. DORTZBACH, *ibid.* **90** (1983) 1066.
8. S. B. HAMMERSCHLAG, S. HUGHES, G. V. O'REILLY and A. L. WEBER, *AJR* **139** (1982) 133.
9. K. DE MAN, Thesis, Bohn, Scheltema & Holkema, Utrecht-Antwerpen, 1982, p. 51.
10. J. A. MAURIELLO Jr, J. C. FLANAGAN and R. G. PEYS-TER, *Ophthalmology* **91** (1984) 102.
11. S. R. SEWALL, F. G. PernoUD and M. J. PernoUD, *J. Oral Maxillofac. Surg.* **44** (1986) 821.
12. B. WEINTRAUB, R. L. CUCIN and M. JACOBS, *Plast. Reconstr. Surg.* **68** (1981) 586.
13. J. A. MAURIELLO, P. M. FIORE and M. KOTCH, *Ophthalmology* **94** (1987) 248.
14. W. D. MORAIN, E. D. COLBY, M. E. STAUFFER, C. L. RUSSEL and D. G. ASTORIAN, *Plast. Reconstr. Surg.* **80** (1987) 769.
15. S. A. BURRES, A. M. COHN and R. H. MATHOG, *The Laryngoscope* **91** (1981) 1881.
16. R. SCHMELZE, in "Fortschritte der Kiefer- und Gesichtschirurgie" Bd. XIX., edited by K. Schuchardt and B. Spiessl (Thieme, Stuttgart-New York, 1975) p. 193.
17. K. DE MAN, Thesis, Bohn, Scheltema & Holkema, Utrecht-Antwerpen, 1982, p. 61.
18. H. H. HÖTTE, in "Orbital fractures" (Van Gorcum & Comp. N. V., Assen, The Netherlands, 1970) p. 235.
19. J. M. CONVERSE, in "Symposium on Plastic Surgery in the Orbital Region", edited by P. Tessier, A. Callahan, J. C. Mustardé and K. E. Salyer (The C.V. Mosby Company, Saint Louis, 1976) p. 79.
20. T. IIZUKA, P. MIKKONEN, P. PAUKKU and C. LINDQVIST, *Int. J. Oral Maxillofac. Surg.* **20** (1991) 83.
21. F. R. ROZEMA, R. R. M. BOS, A. J. PENNINGS and H. W. B. JANSEN, *J. Oral Maxillofac. Surg.* **48** (1990) 1305.
22. E. J. BERGSMA, F. R. ROZEMA, R. R. M. BOS and W. C. DE BRUIJN, *ibid.* **51** (1993) 666.
23. J. E. BERGSMA, W. C. DE BRUIJN, F. R. ROZEMA and R. R. M. BOS, *Biomaterials*, **16** (1995) 25.
24. K. L. GERLACH, Thesis, Carl Hanser Verlag, München-Wien, 1988, p. 31.
25. J. O. HOLLINGER and G. C. BATTISTONE, *Clin. Orthop.* **207** (1986) 290.
26. H. H. HÖTTE, in "Orbital fractures" (Van Gorcum & Comp. N.V., Assen, The Netherlands, 1970) p. 245.
27. R. A. MOSES, P. LURIE and W. J. GRODSKI, in "Basic aspects of glaucoma research", edited by E. Lütjen-Drecoll (FK Schattauer Verlag, Stuttgart-New York, 1982) p. 199.
28. H. J. SIMONSZ, F. HARTING, B. J. DE WAAL and B. W. J. M. VERBEETEN, *Arch. Ophthalmol.* **103** (1985) 124.
29. R. A. MOSES, P. LURIE and R. WETTE, *Invest. Ophthalmol. Vis. Sci.* **22** (1982) 551.
30. R. A. MOSES, P. E. CARNIGLIA, W. J. GRODZKI and J. MOSES, *ibid.* **25** (1984) 989.
31. A. J. OTTO, Thesis, University of Amsterdam, The Netherlands, 1991, p. 101.
32. G. S. PARSONS and R. H. MATHOG, *Arch. Otolaryngol. Head Neck Surg.* **114** (1988) 743.
33. A. JO, V. RIZEN, V. NIKOLIC and B. BANOVIC, *Surg. Radiol. Anat.* **11** (1989) 241.
34. B. SMITH and W. F. REGAN, *Amer. J. Ophthalmol.* **44** (1957) 733.
35. D. E. P. JONES and J. N. G. EVANS, *J. Laryngol.* **81** (1967) 1109.
36. H. H. HÖTTE, in "Orbital fractures" (Van Gorcum & Comp. N.V., Assen, The Netherlands, 1970) p. 17.
37. P. N. MANSON, C. M. CLIFFORD, C. T. SU, N. T. ILIFF and R. MORGAN, *Plast. Reconstr. Surg.* **77** (1986) 193.
38. D. E. CUTRIGHT and E. E. HUNSUCK, *Oral Surg.* **33** (1972) 28.
39. M. C. GUPTA and V. G. DESHMUKH, *Polymer* **24** (1983) 827.
40. M. VERT, P. CHRISTEL, F. CHABOT and J. LERAY, in "Macromolecular biomaterials", edited by G. W. Hastings and P. J. Ducheyne (CRC Press, Boca-Raton, FL, 1984) p. 120.
41. D. W. GRIJPMMA, A. J. NIJENHUIS and A. J. PENNINGS, *Polymer* **31** (1990) 2201.

Received 4 July 1994
and accepted 17 January 1995